ChemComm

COMMUNICATION

View Article Online
View Journal | View Issue

Cite this: *Chem. Commun.*, 2025, **61**, 19092

Received 12th August 2025,
Accepted 21st October 2025

DOI: 10.1039/d5cc04597e

rsc.li/chemcomm

Ammonia reactivity with ferriotetrylenes: a structural snapshot of a highly dynamic process

Phuong Anh Cao,[a] Alice C. Phung,[a] Ella L. Schwirzke,[a] James C. Fettinger,[a] Theo A. H. Rusmore,[a] Kristian L. Mears,*[a] Petra Vasko*[b] and Philip P. Power*[a]

The reaction of ammonia with the ferriotetrylenes Ar′EFeCp(CO)$_2$ (Cp = η^5-C_5H_5; E = Sn(1), Pb(2); Ar′ = −C_6H_3-{C_6H_3-2,6-$^iPr_2$}$_2$) afforded a product interpreted as either a tin amide hydride (3) or a tin ammonia complex, which has a very long Sn–N bond of 2.4289(3), and which readily regenerates 1 and NH_3 under ambient conditions.

Ammonia (NH_3) is a highly valuable chemical feedstock, with 176 million tons being produced *via* the Haber–Bosch process in 2024.[1] Given its relatively low cost and its vital role in plastics and fertilizer production, considerable research has been directed towards the conversion of NH_3 into value-added chemicals (*e.g.*, organoamines).[2–4] Various methods for NH_3 derivatization have been reported,[5,6] among which the use of homogeneous molecular catalysts have shown promise. For example, several transition metal complexes are known to react with NH_3 to generate dihydrogen and transition metal amides.[7–9] However, in some transition metal systems, oxidative addition of NH_3 leads to the formation of a metal amido hydride complex.[10,11] In contrast, main group compounds, especially those incorporating group 14 elements in low-oxidation states have also displayed similar reactivity to transition metals.[12–19] However, until recently, none of these processes were shown to be reversible, but in 2021, Goicoechea and coworkers reported a reversible activation of NH_3 by a geometrically constrained phosphine. This feat relied on a ligand imposed strained coordination at the phosphorus to increase reactivity, and facilitate the addition of NH_3 across a P–N bond.[20] Aldridge and coworkers also showed reversible coordination of NH_3 is possible with the use of a lithium xanthene-linked diphosphine dihydroborate oligomer (based on frustrated P–B Lewis pair type reactivity).[21] In 2023, Long and coworkers characterized a three-dimensional metal–organic framework species that could reversibly bind ammonia to form a one-dimensional coordination polymer.[22]

Despite these findings, relatively few simple compounds are known to provide a direct insertion of an element into an N–H bond under mild conditions. Hadlington and coworkers reported that a germylene-Ni^0 complex undergoes a metathesis reaction involving a Ge–Cl bond with NH_3 to form a Ge–NH_2 complex and HCl.[23] The reverse reaction can be achieved by treating the Ge–NH_2 species with ammonium chloride to regenerate the germylene-Ni^0 starting compound. Breher reported the reversible N–H activation of NH_3 under mild conditions with the use of a so-called hidden frustrated Lewis pair, which consisted of a phosphorus ylide and an aluminium Lewis acid moiety.[24] In addition, we reported previously that a ferriogermylene species displays an irreversible insertion reaction with NH_3 to form a stable germanium amido hydride species (Fig. 1).[25]

In this report, we describe the synthesis and reactivity of the heavier congeners of this ferriotetrylene system, of the formula Ar′EFeCp(CO)$_2$ (E = Sn, **1**; Pb, **2**; Ar′ = −C_6H_3-{C_6H_3-2,6-$^iPr_2$}$_2$) (Fig. 1) with NH_3. Interestingly, we observe highly dynamic behaviour of NH_3 with Ar′SnFeCp(CO)$_2$, **1**, room temperature, leading to the formation of either a ferriostannylene ammonia complex or an inserted tin amido hydride species, Ar′Sn(H)-(NH_2)FeCp(CO)$_2$ **3** (Fig. 1 and 3) which proved difficult to characterise due to spontaneous release of NH_3 from the complex and the reformation of **1**. Compound **3** (Fig. 3) initially appeared to be the first direct experimental illustration of reversible dynamic ammonia activation under near ambient conditions by an unstrained tin species, but due to the extremely lengthened Sn–N bond distance (2.4289(3) Å) and unstable solution-state behaviour, a conclusive assignment proved difficult.

Initially, we synthesized the ferriostannylene **1** by a procedure similar to that described in the literature.[26] In addition, we prepared its lead(II) analogue (compound **2**) in a similar manner (Scheme 1).

Investigation of the reactivity of solutions of **1** or **2** with NH_3 afforded a dramatic color change from green to orange/red for **1**

[a] *Department of Chemistry, University of California, 95616, USA. E-mail: klmears@ucdavis.edu, pppower@ucdavis.edu*
[b] *Department of Chemistry, University of Helsinki, (A. I. Virtasen aukio 1), P.O. Box 55, 00014, Finland. E-mail: petra.vasko@helsinki.fi*

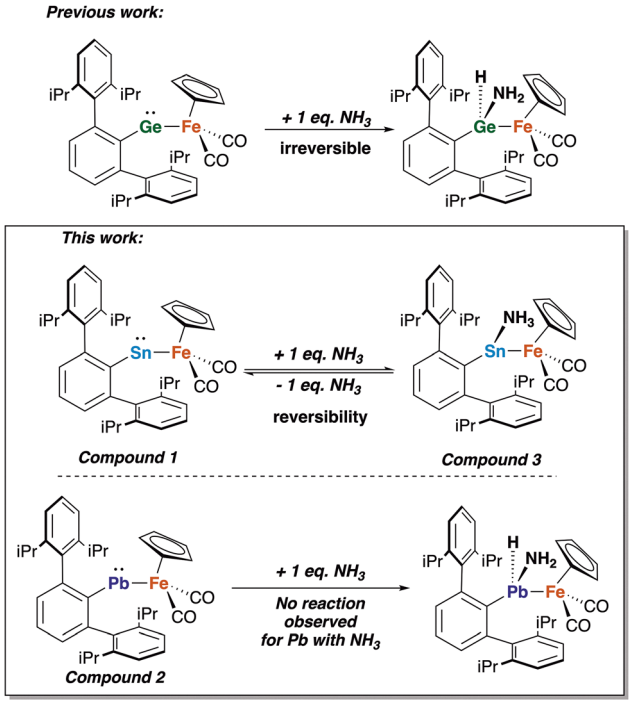

Fig. 1 Overview of the work presented in this study.

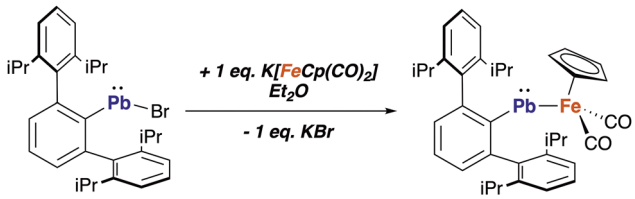

Scheme 1 Synthetic route to compound **2**.

but no change was observed for **2**. We further examined this process for the tin species **1** to determine whether the reaction occurring with NH_3 was a simple coordination of ammonia to Sn or an N–H insertion reaction.

It is worth noting that our previous work on the reactivity of NH_3 with the ferriogermylene analogue of **1** (Fig. 1) revealed that an irreversible insertion into the N–H bond occurs at the tetrel, as it also does for the related diarylstannylene $SnAr'_2$ and diarylgermylene $GeAr'_2$. In the case of the diarylstannylene, reaction with NH_3 afforded the thermodynamically stable tetrel-amido species $[Ar'Sn(\mu\text{-}NH_2)]_2$ *via* elimination of Ar′H. The Ge(IV) amido hydride $Ar'_2Ge(H)NH_2$ was formed from the diarylgermylene, which did not release NH_3, even on heating.[13]

Evidence of N–H bond insertion was attempted *via* the growth of X-ray quality single crystals of **3** (Fig. 2), which were grown by the condensation of pure, anhydrous NH_3 into a forest green solution of **1** in toluene (condensed at *ca.* −78 °C). The resulting orange crystals were initially assigned as the insertion product **3** (Fig. 2). The X-ray data could also be modelled as the NH_3 complex $Ar'Sn(NH_3)FeCp(CO)_2$ to a similar residual value, but in this case, all the ammonia hydrogens

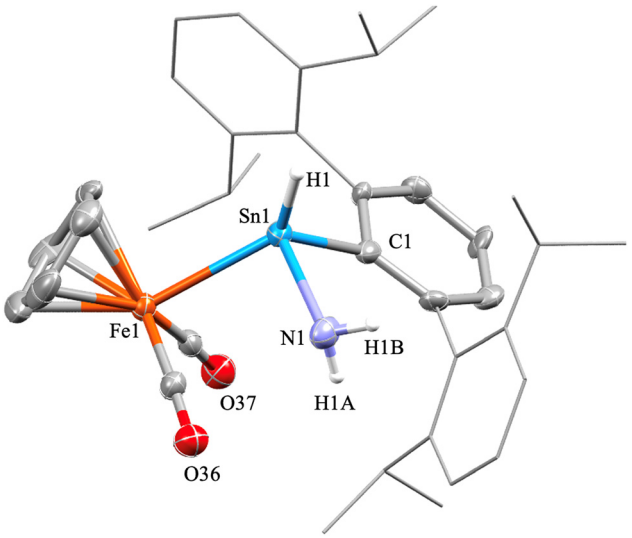

Fig. 2 Molecular structure of compound **3** (thermal ellipsoids are shown at 50% probability). The 2,6-diisopropylphenyl groups are shown in wire-frame format and the H-atoms (except those of the amido group and the tin hydride moieties) are not shown for clarity. Color code: carbon = grey, iron = orange, oxygen = red and tin = blue, nitrogen = lilac, hydrogen = white.

could not be located on a difference map. At room temperature, under ambient conditions, it was observed that the orange crystals returned to their initial green color (*i.e.* **1**) within *ca.* 10 minutes, with liberation of NH_3.

Compound **3** has a distorted tetrahedral coordination at the tin atom. The most striking structural feature is the lengthened Sn1–N1 bond which is 2.4289(3) Å. This is longer than any Sn–N bond distance previously reported for either a Sn–(NH_3) complex or a Sn–NH_2 amido species and may suggest an assignment of an ammonia complex, over an inserted product.[27] This may be contrasted with the related germanium amido hydride compound $Ar'Ge(NH_2)(H)FeCp(CO)_2$ and $Ar^{\#}Ge(NH_2)(H)FeCp(CO)_2$ ($Ar^{\#}$ = C_6H_3-2,6-{C_6H_2-2,4,6-Me_3}$_2$), whose bonds show only a small dependence on the type of terphenyl substituent employed (1.8505(2) Å for the Ge–N bond in $Ar^{\#}Ge(NH_2)(H)FeCp(CO)_2$ and 1.757(4) Å in $Ar'Ge(NH_2)(H)FeCp(CO)_2$).[12] These variations are obviously far smaller than those seen for **3**, which further highlights its unique structure. However, it could be that the structure obtained is indicative of the weakening Sn–NH_2 bond within a ammonia-inserted ferriostannylene **3** and the incipient formation of a complexed NH_3 moiety, which rapidly dissociates. As crystal selection was occurring at room temperature, rapid NH_3 loss from the sample was clear, particularly in the colour change from orange back to green, Thus, the X-ray data for **3** could be considered as a structural snapshot of a reversible NH_3 insertion and regeneration of **1** at ambient temperature (as shown in Fig. 2).

The Sn1–C1 bond length 2.2921(3) Å of **3** is comparable to that of the Sn1–C1 bonds (2.240(3) Å) in compound **1** (2.208(3) Å), as well as those in the diarylstannylene bridged amide (2.240(3) Å) $[Ar'Sn(\mu\text{-}NH_2)]_2$.[13] The Sn1–Fe1 distance in **3** (2.6703(4) Å) is far longer than the Sn1–Fe1 distance observed in the starting material

1 (2.6040(16) Å). The C1–Sn1–Fe1 angle (109.13(5)°) in **3** is slightly narrower than the corresponding angle in compound **1** (112.65(9)°), due to the increased coordination number.

To further pin down the identity of compound **3**, we attempted variable temperature NMR experiments by the condensation of dried NH_3 into a J. Young NMR tube containing a solution of **1** in C_7D_8. This experiment yielded a change in the chemical shift of the ^{119}Sn NMR signal, from δ_{Sn} = 2958.6, which corresponds to the parent ferriostannylene, to a broadened δ_{Sn} = 752.2 at 293 K, which we assign to a dynamic coordination of NH_3 to **1**.[28] The signal shifted further upfield to 557.9 ppm when the temperature was decreased to 193 K, which resembles more of a Sn(IV) signal, and could allude to the insertion pathway. A ^{1}H-coupled ^{119}Sn NMR spectrum of **3** did not show clear coupling (*cf.* Fig. S9). A coupling consistent with a four-coordinate Sn(IV) complex could be expected to be in the range of $^1J(^{119}Sn–^1H)$ = 103.13 Hz.[28,29] The ^{1}H NMR spectrum also revealed a broad signal at −0.05 ppm, which is caused by the dynamic coordination of free and complexed NH_3. The ^{1}H VT NMR studies further showed a change of the broad singlet to a sharper signal at −0.09 ppm at 213 K and then finally to a narrow signal with a chemical shift at −0.12 ppm at 193 K. The upfield shift at lower temperatures again made an assignment of either the inserted amide product or an ammonia complex difficult. Additionally, a broad signal detected at 2.97 ppm could potentially be assigned as the Sn–H group, though a signal that could reasonably be assigned to the Sn–NH_2 resonance was not observed.

Despite the VT-NMR experiments, the results of a van't Hoff analysis proved insufficiently definitive to determine very accurate energy values, as the concentration of ammonia was difficult to measure with our equipment, and the highly unstable nature of the coordination rendered FTIR experiments with our setup impossible. Instead, the feasibility of an insertion mechanism was probed using density function theory (DFT). The DFT calculations indicated that indeed, the first step of an activation process is the complexation of an NH_3 molecule to the unoccupied, virtually pure 5p orbital of the tin atom giving the ammonia adduct (**Int1**, Fig. 3). This is followed by the association of three NH_3 molecules *via* N–H interactions with the complexed NH_3, which facilitates Sn–H and Sn–NH_2 formation *via* a concerted process (**TS1**, Fig. 3).

These results indicate that at room temperature, the reaction is essentially thermoneutral, with reaction energy barriers consistent with the observed X-ray and spectroscopic data. At lower temperatures, the insertion becomes slightly exergonic despite the lower entropy value. A similar mechanism has been calculated for a diarylgermylene complex reacting with hydrazines as reported earlier.[30]

For the ferrioplumblyene species (compound **2**), dark green crystals of **2** (60% yield) were characterized by single crystal X-ray diffraction (Fig. 4) which showed the expected, bent two coordinate geometry at lead with a Fe1–Pb1–C1 angle of 111.09(16)°.[31] The Fe1–Pb1 bond length in **2** is 2.6388(11) Å, which is shorter than the bond length (2.7367(5) Å) of a plumbylone complex reported by Driess and coworkers, which

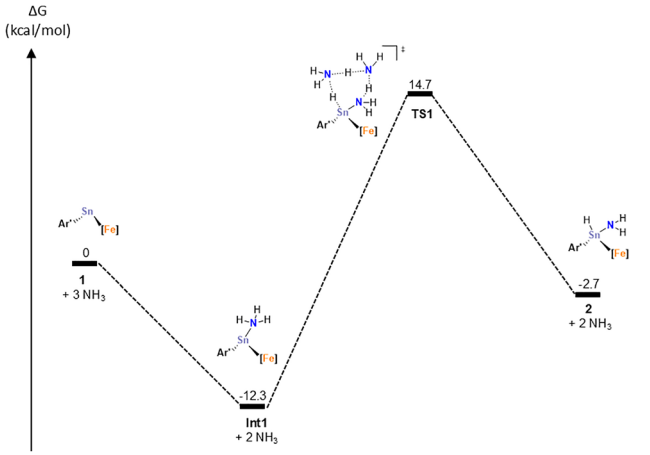

Fig. 3 DFT-calculated reaction profile between Ar′SnFeCp(CO)$_2$ (**1**) and 3 molecules of NH_3 to give **3** at 193 K (red) in 1 atm ([Fe] = FeCp(CO)$_2$ and Ar′ = −C_6H_3-{C_6H_3-2,6-^{i}Pr$_2$}$_2$). Calculated at the SMD-PBE0-GD3BJ/Def2-TZVP//PBE0-GD3BJ/Def2-SVP/Def2 TZVP(Sn,Fe) level of theory. Energies represent Gibbs free energies (kcal mol^{-1}) in 1 atm at the given temperature.

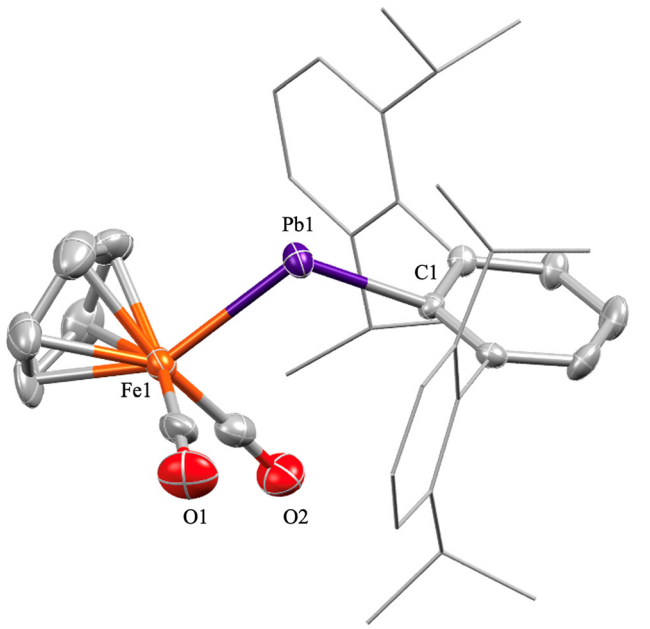

Fig. 4 Molecular structure of compound **2** (thermal ellipsoids are shown at 50% probability). The 2,6-diisopropylphenyl groups are shown in wire-frame format and H-atoms are not shown for clarity. Color code: carbon = grey, iron = orange, oxygen = red and lead = and lead = purple.

has the formula {[Si^{II}(Xant)Si^{II}]Pb^{0}Fe(CO)$_4$} (Si^{II}(Xant)Si^{II} = PhC(N*t*Bu)$_2$Si-(Xant)Si(N*t*Bu)$_2$CPh).[32] In Driess' compound, the lead atom also coordinates datively to the tetracarbonyl iron. The Pb1–C1 bond length (2.321(6) Å) in **2** is comparable to those (2.313(13) Å and 2.307(13) Å) in the ferrioplumbylene species of formula Fe(CO)$_4$(PbAr*)$_2$ (Ar* = −C_6H_3-2,6-{C_6H_2-2,4,6-^{i}Pr$_3$}$_2$) reported earlier by our group.[33]

The ^{207}Pb NMR spectrum of **2** at 298 K shows a signal at 11724.1 ppm, which lies in the expected region for a two-

coordinate Pb(II) complex.[34] In addition, the ^{1}H NMR spectrum displayed the expected signals, from the η^5-C_5H_5 Cp protons (4.18 ppm) and 2,6-diisopropyl methyl protons (1.12 ppm and 1.39 ppm). UV-Vis spectroscopy of **2** showed λ_{max} absorbances at 337 nm ($\pi \rightarrow \pi^*$ transition) and 634 nm ($n \rightarrow \pi^*$ transition). FTIR spectroscopic analysis showed CO stretches at n_{CO} = 1961 and 1916 cm^{-1}.

In summary, we report the synthesis and characterisation of the heavier congeners of a ferriotetrylene system of the formula Ar′EFeCp(CO)$_2$ (Cp = η^5-C_5H_5; E = Sn(1), Pb(2); Ar′ = −C_6H_3-{C_6H_3-2,6-^{i}Pr$_2$}$_2$) and probed their reactivity with ammonia. The ferriostannylene **1** afforded, at the least, coordination of ammonia to the Sn atom in **1** as determined using single crystal X-ray diffraction and multinuclear VT-NMR experiments, but the extent as to which an insertion into the N–H bond of NH_3 proved difficult to determine due to low energy barriers for both mechanisms, as calculated using DFT. However, the reactivity of **1** with NH_3 lies between the profiles of its lighter and heavier congeners. The analogous ferriogermylene irreversibly inserts into the N–H bond of ammonia, and the ferrioplumbylene **2** is unreactive with NH_3. Based on the crystallographic evidence for **3**, the Sn–N bond distance is elongated due low energy barriers for both the coordination, insertion and liberation of NH_3 at ambient temperature and pressure. This structure provides an insight into NH_3 coordination at **1** and may provide a unique view into a dynamic process of reversible N–H bond scission and subsequent NH_3 regeneration at a main group metal. This study further provides a complete picture of ferriotetrylene reactivity with ammonia, which could inform future catalyst design for small molecule activation. The activation of other industrially relevant small molecules using this ferriostannylene complex is currently in hand.

Conflicts of interest

There are no conflicts to declare.

Data availability

The data supporting this article have been included as part of the supplementary information (SI). Supplementary information is available. The SI includes synthetic procedures and analyses of the compounds. See DOI: **https://doi.org/10.1039/d5cc04597e**.

CCDC 2248740 (**2**) and 2468055 (**3**) contain the supplementary crystallographic data for this paper.[35a,b]

Notes and references

1 N. Salmon and R. Bañares-Alcántara, *Sustainable Energy Fuels*, 2021, **5**, 2814–2839.
2 J. Hoover, *Science*, 2016, **354**, 707–708.
3 A. S. Guram, R. A. Rennels and S. L. Buchwald, *Angew. Chem., Int. Ed. Engl.*, 1995, **34**, 1348–1350.
4 J. Louie and J. F. Hartwig, *Tetrahedron Lett.*, 1995, **36**, 3609–3612.
5 J. I. van der Vlugt, *Chem. Soc. Rev.*, 2010, **39**, 2302.
6 S. Streiff and F. Jérôme, *Chem. Soc. Rev.*, 2021, **50**, 1512–1521.
7 J. L. Klinkenberg and J. F. Hartwig, *J. Am. Chem. Soc.*, 2010, **132**, 11830–11833.
8 M. J. Bezdek, S. Guo and P. J. Chirik, *Science*, 2016, **354**, 730–733.
9 Y. Nakajima, H. Kameo and H. Suzuki, *Angew. Chem., Int. Ed.*, 2006, **45**, 950–952.
10 J. Zhao, A. S. Goldman and J. F. Hartwig, *Science*, 2005, **307**, 1080–1082.
11 E. Morgan, D. F. MacLean, R. McDonald and L. Turculet, *J. Am. Chem. Soc.*, 2009, **131**, 14234–14236.
12 Y. Peng, J.-D. Guo, B. D. Ellis, Z. Zhu, J. C. Fettinger, S. Nagase and P. P. Power, *J. Am. Chem. Soc.*, 2009, **131**, 16272–16282.
13 Y. Peng, B. D. Ellis, X. Wang and P. P. Power, *J. Am. Chem. Soc.*, 2008, **130**, 12268–12269.
14 S. L. McOnie, G. A. Özpınar, J. L. Bourque, T. Müller and K. M. Baines, *Dalton Trans.*, 2021, **50**, 17734–17750.
15 D. Sarkar, P. Vasko, L. Ying, J. J. C. Struijs, L. P. Griffin and S. Aldridge, *Angew. Chem., Int. Ed.*, 2025, **64**, e202502326.
16 Z. Zhu, X. Wang, Y. Peng, H. Lei, J. C. Fettinger, E. Rivard and P. P. Power, *Angew. Chem., Int. Ed.*, 2009, **48**, 2031–2034.
17 D. M. J. Krengel, N. Graw, R. Herbst-Irmer, D. Stalke, O. P. E. Townrow and M. Fischer, *Inorg. Chem. Front.*, 2024, **11**, 8649–8659.
18 D. C. H. Do, A. V. Protchenko, M. Á. Fuentes, J. Hicks, P. Vasko and S. Aldridge, *Chem. Commun.*, 2020, **56**, 4684–4687.
19 J. Cui, Y. Li, R. Ganguly, A. Inthirarajah, H. Hirao and R. Kinjo, *J. Am. Chem. Soc.*, 2014, **136**, 16764–16767.
20 J. Abbenseth, O. P. E. Townrow and J. M. Goicoechea, *Angew. Chem., Int. Ed.*, 2021, **60**, 23625–23629.
21 A. E. Crumpton, A. Heilmann and S. Aldridge, *Angew. Chem., Int. Ed.*, 2024, 63.
22 B. E. R. Snyder, A. B. Turkiewicz, H. Furukawa, M. V. Paley, E. O. Velasquez, M. N. Dods and J. R. Long, *Nature*, 2023, **613**, 287–291.
23 P. M. Keil, T. Szilvási and T. J. Hadlington, *Chem. Sci.*, 2021, **12**, 5582–5590.
24 F. Krämer, J. Paradies, I. Fernández and F. Breher, *Nat. Chem.*, 2024, **16**, 63–69.
25 A. C. Phung, J. C. Fettinger and P. P. Power, *Organometallics*, 2021, **40**, 3472–3479.
26 H. Lei, J.-D. Guo, J. C. Fettinger, S. Nagase and P. P. Power, *Organometallics*, 2011, **30**, 6316–6322.
27 A. V. Protchenko, J. I. Bates, L. M. A. Saleh, M. P. Blake, A. D. Schwarz, E. L. Kolychev, A. L. Thompson, C. Jones, P. Mountford and S. Aldridge, *J. Am. Chem. Soc.*, 2016, **138**, 4555–4564.
28 B. Wrackmeyer, *^{119}Sn-NMR Parameters, Annual Reports on NMR Spectroscopy*, Elsevier, 1985, vol. 16, pp 73–186, DOI: **10.1016/S0066-4103(08)60226-4**.
29 A. G. Davies, *Organotin Chemistry*, 2nd edn, Wiley-VCH, 2004, p. 18.
30 Z. D. Brown, J.-D. Guo, S. Nagase and P. P. Power, *Organometallics*, 2012, **31**, 3768–3772.
31 C. Stanciu, S. S. Hino, M. Stender, A. F. Richards, M. M. Olmstead and P. P. Power, *Inorg. Chem.*, 2005, **44**, 2774–2780.
32 J. Xu, S. Pan, S. Yao, G. Frenking and M. Driess, *Angew. Chem., Int. Ed.*, 2022, **61**, e202209442.
33 Q. Zhu, J. C. Fettinger, P. Vasko and P. P. Power, *Organometallics*, 2020, **39**, 4629–4636.
34 B. Wrackmeyer, *^{207}Pb-NMR Parameters, Annual Reports on NMR Spectroscopy*, Elsevier, 1990, vol. 22, pp 249–306, DOI: **10.1016/S0066-4103(08)60257-4**.
35 (*a*) CCDC 2248740: Experimental Crystal Structure Determination, 2025, DOI: **10.5517/ccdc.csd.cc2fh00z**; (*b*) CCDC 2468055: Experimental Crystal Structure Determination, 2025, DOI: **10.5517/ccdc.csd.cc2nv6pf**.